Tryptamine–Triazole Hybrid Compounds for Selective Butyrylcholinesterase Inhibition

Minky Son,[†,†] Haneul Lee,[‡,†] Cheolmin Jeon,[‡] Yujung Kang,[‡] Chanin Park,[‡] Keun Woo Lee,[†,*] and Jeong Ho Park[‡,*]

[†]*Division of Life Science, Division of Applied Life Science (BK21 Plus), Plant Molecular Biology and Biotechnology Research Center (PMBBRC), Systems and Synthetic Agrobiotech Center (SSAC), Research Institute of Natural Science (RINS), Gyeongsang National University (GNU), Jinju 52828, Republic of Korea. *E-mail: kwlee@gnu.ac.kr*

[‡]*Department of Chemical & Biological Engineering, Hanbat National University, Daejeon 34158, South Korea. *E-mail: jhpark@hanbat.ac.kr*

[†]*These authors contributed equally to this work.*

Received February 23, 2019, Accepted March 29, 2019

Tryptamine–triazole hybrid compounds (**11**–**18**) were synthesized via click reaction between tryptamine azide and propargylated natural compounds. Their cholinesterase inhibitory activity was evaluated. Among the eight compounds, compound **11** showed the most potent inhibitory activity [IC_{50} = 0.42 ± 0.29 μM for equine butyrylcholinesterase (BuChE) and 1.96 ± 0.15 μM for human BuChE]. From the molecular modeling study, compound **11** was bound to the catalytic anionic site, anionic subsite, peripheral anionic subsite, acyl-binding pocket, and oxyanion hole of human or horse BuChE by forming a hairpin or U-shaped structure. The Lineweaver-Burk plot of compound **11** against BuChE suggests a mixed type of inhibition which corresponds well with the molecular modeling study.

Keywords: Tryptamine–triazole hybrid compounds, Cholinesterase inhibitory activity, Alzheimer's disease, Molecular docking calculation, Molecular dynamics simulation

Introduction

For the last 10 years, new drugs have not been introduced to the market for Alzheimer's disease (AD) treatment. Therefore, strategies are needed to develop drug candidates for AD. There are many targets for AD drugs such as beta-amyloid, tau-protein, cholinesterase, γ- and β-secretase, neurotransmitter systems (serotoninergic 5-HT_6 and histaminergic H_3), etc.[1] Among them, cholinesterase inhibitors based on the cholinergic hypothesis are still the most valuable targets for novel AD drugs.[2] Currently commercially available AD drugs such as donepezil, rivastigmine, and galantamine are targeted primarily to acetylcholinesterase (AChE). However, they are not a complete remedy for AD and have many side effects that require a new type of target for cholinergic hypothesis. The activity of AChE in AD patients is decreases but that of BuChE is increased to 40–90%.[3,4] When a selective inhibitor of BuChE, such as a cymserine analogue, is applied to rodents, the concentration of acetylcholine (ACh) in the brain increases.[4] Thus, selective inhibition of BuChE may increase ACh levels in AD patients with superior drug candidates.

Synthesis of derivatives of natural or secondary metabolites with physiological activities such as antioxidant, anti-inflammatory, or cytoprotective and verifying that they meet cholinergic hypothesis can be a good strategy for developing AD therapeutic compounds. In this study, we have synthesized derivatives of natural compounds such as lipoic acid, polyphenols, or paeonol with various physiological activities and studied whether they can act as selective BuChE inhibitors.

α-Lipoic acid (ALA) and its reduced form, dihydrolipoic acid, show various physiological activities. ALA is often referred to as an "antioxidant of antioxidants" because of its ability to act as a multifunctional antioxidant against a variety of reactive oxygen species (ROS)[5,6] and to promote new synthesis of endogenous antioxidants such as glutathione, α-tocopherol, and vitamin C.[5] ALA conjugated compounds such as ALA-tacrin conjugate (Lipocrine; IC_{50} = 6.96 ± 0.45 nM for AChE)[7] and ALA-triazole-coumarin conjugate (IC_{50} = 7.8 ± 3.6 μM for BuChE)[8] showed cholinesterase inhibitory activity.

Natural polyphenols (PPs) are known as natural antioxidants by reducing ROS levels *in vivo*.[9] PP also reduces the inflammation effect on coronary artery disease[10] and slows down the process of wrinkling the skin.[11]

Paeonol is a natural compound isolated from *Paeonia suffruicosa*.[12] Paeonol and its derivatives have many beneficial anticancer, antimicrobial, antimutagenic, anti-inflammatory, and analgesic properties.[13]

Previously, we have reported that a benzoisoxazole-tryptamine hybrid compound (**1**) showed good BuChE

inhibitory value (IC_{50} = 0.72 ± 0.11 μM) (Figure 1).[14] In this study, compound **1** derivatives were synthesized by converting the benzoisoxazole moiety to biologically active natural compounds. The click reaction between trytamine azide and propargylated lipoic acid, polyphenols, and paeonol was carried out. We also evaluated the effect of compound **1**-derivatives on BuChE inhibition *in vitro*. Molecular modeling studies using compound **11** in human or horse BuChE have been performed to understand the binding mode.

Experimental

General Methods. ^{1}H NMR and ^{13}C NMR spectra were recorded on a Varian Mercury 400 (400 MHz) spectrometer (Varian, Palo Alto, California, USA) and mass spectra were taken using an Agilent G1956B mass spectrometer (Agilent, Santa Clara, California, USA). Flash column chromatography was performed using E. Merck silica gel (60, particle size 0.040–0.063 mm) and analytical thin layer chromatography (TLC) was performed using pre-coated TLC plates with silica gel 60 F254 (Merck, Merck, Darmstadt, Germany). The microwave synthesis reaction was carried out using a Biotage microwave reactor (Model: Initiator Exp Eu, Sweden). Unless otherwise noted, the reagents used were reagent grade and all synthetic reactions were carried out under an argon atmosphere using a dry solvent. (α)-Lipoic acid was purchased from Xi'an Union Pharmpro Co., Ltd., (Xi'an, China). Caffeic acid, 3,4-dimethoxy cinnamic acid, ferulic acid, syringic acid, honokiol, 2,4-dihydroxyacetophenone, acetic anhydride, *N,N*-dimethylpyridin-4-amine (DMAP), *N*-(3-dimethylaminopropyl)-N′-ethylcarbodiimide hydrochloride (EDC), triethylamine (TEA), Cs_2CO_3, PPh_3, H_3PO_4, KI, NaOH, acetylcholinesterase [electric eel, cat. (C2888)], and butyrylcholinesterase [equine serum, cat. (C-7512) and human serum, cat. (B4168)] were purchased from Sigma-Aldrich Korea (Yongin, Korea), Merck, or ThermoFisher Scientific (Seoul, Korea) and used without purification.

General Synthetic Procedure

General Procedure (A). The following is a general reaction procedure for the synthesis of propargylated derivatives (**3**, **7**–**10**). EDC (1.5 equiv), hydroxybenzotriazole (HOBT, 0.1 equiv), and propargylamine (1.1 equiv) were added at room temperature to a dichloromethane (DCM) solution of the carboxylic acids. The reaction mixture is stirred at room temperature for 4 h and then water is added. The solution was extracted three times with DCM and dried over anh. $MgSO_4$. The solvent was removed *in vacuo* and the residue was purified by silica gel column chromatography (DCM: EA = 4: 1) to give the propargylated compound (**3**, **7**–**10**).

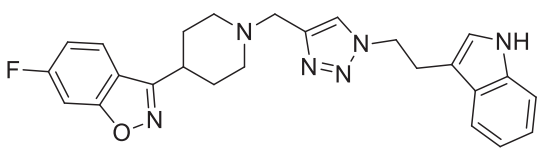

1. IC_{50} = 0.72 ± 0.11 μM for eq.BuChE

Figure 1. Structures of benzoisoxazole moiety-tryptamine hybrid compound (**1**).

General Procedure (B). The following is a general reaction procedure for the synthesis of propargylated derivatives (**5** and **6**). Propargyl bromide (1.5 equiv) was added to the mixture of 2,4-dihydroxyacetophenone or paeonol (1.1 equiv), and Cs_2CO_3 (1.1 equiv) in acetone at room temperature. The reaction mixture was refluxed for 24 h and water was added. The solution was extracted three times with DCM and dried over anh. $MgSO_4$. The solvent was removed *in vacuo*, and the residues were purified by silica gel column chromatography (EA: Hex = 1: 6) to give propargylated compounds (**5** and **6**), respectively.

General Procedure (C). The following is a general reaction procedure for the synthesis of compound (**1**)-derivatives by the click reaction using a microwave reactor. Tryptamine azide (**2**, 1.1 equiv) was prepared by treating tryptamine with imidazole sulfonyl azide,[15] which was added to a solution of propargylated compounds (**3**–**10**, 1.0 equiv) in acetone in the presence of $Cu(PPh_3)_3Br$ (0.1 equiv).[16] The reaction mixture was reacted in a microwave reactor at 65 °C for 30 min and then water was added. The solution was extracted three times with DCM and dried over anh. $MgSO_4$. The solvent was removed *in vacuo* and the tryptamine derivatives (**11**–**18**) were purified using silica gel column chromatography (DCM: MeOH = 9: 1), respectively.

*(R)-N-((1-(2-(1H-indol-3-yl)ethyl)-1H-1,2,3-triazol-4-yl) methyl)-5-(1,2-dithiolan-3-yl)pentanamide (**11**).* Click reaction between compounds **3** and **2** resulted in compound **11** with 89% yield via general procedure (**C**).

Compound **3**: White solid; yield: 85%; ^{1}H NMR (400 MHz, $CDCl_3$): δ 1.43 (m, 2H), 1.64 (m, 4H), 1.87 (m, 1H), 2.16 (m, 3H), 2.41 (m, 1H), 3.27 (m, 2H), 3.76 (m, 1H), 4.01 (m, 2H), 5.56 (s, 1H).

Compound **11**: Yellow oily product; yield: 89%; ^{1}H NMR (400 MHz, $CDCl_3$): δ 1.38 (m, 2H), 1.62 (m, 4H), 1.85 (m, 1H), 2.12 (t, *J* = 7.2 Hz, 2H), 2.43 (m, 1H), 3.09 (m, 2H), 3.33 (t, *J* = 6.8 Hz, 2H), 3.51 (m, 1H), 4.38 (d, *J* = 5.6 Hz, 2H), 4.60 (t, *J* = 6.8 Hz, 2H), 6.15 (s, 1H), 6.87 (s, 1H), 7.08 (t, *J* = 8.0 Hz, 1H), 7.18 (t, *J* = 8.0 Hz, 1H), 7.19 (s, 1H), 7.36 (d, *J* = 8.0 Hz, 1H), 7.43 (t, *J* = 8.0 Hz, 1H), 8.24 (s, 1H); ^{13}C NMR (100 MHz, DMSO-d_6): δ 25.3, 26.5, 28.8, 34.5, 34.8, 36.0, 38.4, 40.2, 50.9, 56.4, 110.6, 111.6, 118.1, 119.3, 122.0, 122.8, 122.9, 126.9, 136.3, 144.5, 173.2; ESI-MS: *m/z* $[M]^+$ 460.63 (calcd 460.1).

*(R)-1-(4-(1,2-dithiolan-3-yl)butyl)-3-((1-(2-(1H-indol-3-yl) ethyl)-1H-1,2,3-triazol-4-yl)methyl)urea (**12**).* Compound

4 was synthesized by Curtius rearrangement of lipoic acid using diphenyl phosphorazidate (1.0 equiv) and propargyl amine. Click reaction between compound **4** and **2** resulted in compound **12** with 89% yield via general procedure (**C**).

Compound **4**: White solid; yield: 87%; ^{1}H NMR (400 MHz, $CDCl_3$): δ 1.45 (m, 4H), 1.65 (m, 3H), 1.89 (m, 1H), 2.18 (s, 1H), 2.43 (m, 1H), 3.07 (m, 2H), 3.19 (m, 2H), 3.50 (m, 1H), 3.94 (m, 2H), 4.65 (bs, 1H), 4.73 (bs, 1H).

Compound **12**: Yellow oily product; yield: 89%; ^{1}H NMR (400 MHz, DMSO-d_6): δ 1.30 (m, 3H), 1.48 (m, 1H), 1.60 (m, 1H), 1.81 (m, 1H), 2.34 (m, 1H), 2.93 (m, 2H), 3.06 (m, 1H), 3.11 (m, 1H), 3.18 (t, J = 7.6 Hz, 2H), 3.54 (m, 1H), 4.14 (d, J = 5.6 Hz, 2H), 4.54 (t, J = 7.6 Hz, 2H), 5.88 (t, J = 5.6 Hz, 1H), 6.17 (t, J = 5.6 Hz, 1H), 6.93 (t, J = 7.4 Hz, 1H), 7.02 (t, J = 7.4 Hz, 1H), 7.05 (d, J = 2.4 Hz, 1H), 7.28 (d, J = 8.0 Hz, 1H), 7.49 (d, J = 8.0 Hz, 1H), 7.65 (m, 1H), 7.85 (s, 1H), 10.82 (s, 1H); ^{13}C NMR (100 MHz, $CDCl_3$): δ 21.61, 25.16, 25.20, 29.73, 29.73, 30.64, 33.62, 35.28, 35.42, 45.99, 51.75, 105.72, 106.82, 113.26, 114.61, 117.24, 118.14, 121.97, 125.08, 128.53, 131.48, 153.97; ESI-MS: *m/z* $[M]^+$ 445.1 (calcd 445.1).

*1-(4-((1-(2-(1H-indol-3-yl)ethyl)-1H-1,2,3-triazol-4-yl) methoxy)-2-hydroxyphenyl)ethenone (**13**).* Click reaction between compounds **5** and **2** resulted in compound **13** with 79% yield via general procedure (**C**). Analytical data can be found in Ref. 17.

*1-(2-((1-(2-(1H-indol-3-yl)ethyl)-1H-1,2,3-triazol-4-yl) methoxy)-4-methoxyphenyl)ethenone (**14**).* Click reaction between compounds **6** and **2** resulted in compound **14** with 92% yield via general procedure (**C**). Analytical data can be found in Ref. 17.

*4-((1-(2-(1H-indol-3-yl)ethyl)-1H-1,2,3-triazol-4-yl) methylcarbamoyl)-2,6-dimethoxyphenyl acetate (**15**).* Click reaction between compound **7** and **2** resulted in compound **15** with 70% yield via general procedure (**C**). Analytical data can be found in Ref. 17.

*(E)-N-((1-(2-(1H-indol-3-yl)ethyl)-1H-1,2,3-triazol-4-yl) methyl)-3-(3,4-dimethoxyphenyl)acrylamide (**16**).* Click reaction between compounds **8** and **2** resulted in compound **16** with 85% yield via general procedure (**C**).

Compound **8**: Analytical data can be found in Ref. 14.

Compound **16**: White solid; yield: 85%; ^{1}H NMR (400 MHz, DMSO-d_6): δ 3.19 (t, J = 7.6 Hz, 2H), 3.73 (s, 6H), 4.35 (d, J = 2.4 Hz, 2H), 4.55 (t, J = 7.6 Hz, 2H), 6.49 (d, J = 15.6 Hz, 1H), 6.93 (s, J = 4.0 Hz, 1H), 6.94 (s, 1H), 7.02 (t, J = 7.6 Hz, 1H), 7.05 (d, J = 12.0 Hz, 1H), 7.06 (s, 1H), 7.08 (d, J = 12.0 Hz, 1H), 7.28 (d, J = 7.6 Hz, 1H), 7.39 (d, J = 15.6 Hz, 1H), 7.49 (d, J = 7.6 Hz, 1H), 7.95 (s, 1H), 8.42 (t, J = 2.4 Hz, 1H), 10.83 (s, 1H); ^{13}C NMR (100 MHz, DMSO-d_6): δ 26.5, 34.8, 50.3, 55.8, 56.0, 110.5(2C), 111.9. 112.2, 118.6, 118.9, 120.1, 121.5, 121.7, 123.3, 123.6, 127.3, 128.1, 136.6, 139.5, 145.1, 149.3, 150.6, 165.6; ESI-MS: *m/z* $[M]^+$ 432.49 (calcd 432.2); mp: 160 °C.

*4-((E)-2-((1-(2-(1H-indol-3-yl)ethyl)-1H-1,2,3-triazol-4-yl) methylcarbamoyl)vinyl)-2-methoxyphenyl acetate (**17**).* Click reaction between compounds **9** and **2** resulted in compound **17** with 95% yield via general procedure (**C**).

Compound **9**: Yellow solid; yield: 66%; ^{1}H NMR (400 MHz, $CDCl_3$): δ 1.99 (d, J = 2.8 Hz, 1H), 2.25 (s, 3H), 3.82 (s, 3H), 4.16 (q, J = 2.8 Hz, 2H), 5.93 (bs, 1H), 6.30 (d, J = 15.2 Hz, 1H), 7.01 (d, J = 8.4 Hz, 1H), 7.03 (d, J = 4.4 Hz, 1H), 7.06 (dd, J = 8.8, 4.4 Hz, 1H), 7.57 (d, J = 15.2 Hz, 1H).

Compound **17**: White solid; yield: 95%; ^{1}H NMR (400 MHz, DMSO-d_6): δ 2.24 (s, 3H), 3.22 (t, J = 7.5 Hz, 2H), 3.78 (s, 3H), 4.39 (d, J = 5.2 Hz, 2H), 4.58 (t, J = 7.5 Hz, 2H), 6.63 (d, J = 15.6 Hz, 1H), 6.95 (t, J = 7.2 Hz, 1H), 7.04 (t, J = 7.2 Hz, 1H), 7.08 (d, J = 6.8 Hz, 1H), 7.10 (s, 1H), 7.13 (d, J = 6.8 Hz, 1H), 7.28 (s, 1H), 7.30 (d, J = 8.0 Hz, 1H), 7.42 (d, J = 15.6 Hz, 1H), 7.51 (d, J = 8.0 Hz, 1H), 8.10 (s, 1H), 8.54 (t, J = 5.2 Hz, 1H), 10.84 (s, 1H); ^{13}C NMR (100 MHz, DMSO-d_6): δ 20.8, 26.49, 34.83, 50.37, 56.20, 110.45, 111.85, 112.04, 118.63, 118.85, 120.41, 121.50, 122.68, 123.57, 123.72, 127.32, 134.32, 136.56, 138.81, 140.58, 151.48, 165.22, 168.88; ESI-MS: *m/z* $[M]^+$ 460.5 (calcd 460.1); mp: 175 °C.

*4-((E)-2-((1-(2-(1H-indol-3-yl)ethyl)-1H-1,2,3-triazol-4-yl) methylcarbamoyl)vinyl)phenyl-1,2-diacetate (**18**).* Click reaction between compounds **10** and **2** resulted in compound **18** with 70% yield via general procedure (**C**).

Compound **10**: White solid; yield: 20%; ^{1}H NMR (400 MHz, $CDCl_3$): δ 2.20 (d, J = 2.8 Hz, 1H), 2.26 (s, 6H), 4.13 (q, J = 2.8 Hz, 2H), 5.86 (bs, 1H), 6.25 (d, J = 15.6 Hz, 1H), 7.14 (d, J = 8 Hz, 1H), 7.28 (d, J = 2 Hz, 1H), 7.31 (dd, J = 8, 2 Hz, 1H), 7.53 (d, J = 15.6 Hz, 1H).

Compound **18**: White solid; yield: 70%; ^{1}H NMR (400 MHz, DMSO-d_6): δ 2.26 (s, 6H), 3.22 (t, J = 7.6 Hz, 2H), 4.38 (d, J = 5.7 Hz, 2H), 4.58 (t, J = 7.6 Hz, 2H), 6.61 (d, J = 15.6 Hz, 1H), 6.95 (t, J = 7.5 Hz, 1H), 7.03 (t, J = 7.5 Hz, 1H), 7.08 (s, 1H), 7.28 (d, J = 7.5 Hz, 1H), 7.30 (d, J = 7.5 Hz, 1H), 7.41 (d, J = 15.6 Hz, 1H), 7.44 (s, 1H), 7.47 (d, J = 8.0 Hz, 1H), 7.51 (d, J = 8.0 Hz, 1H), 7.97 (s, 1H), 8.58 (t, J = 5.7 Hz, 1H), 10.83 (s, 1H); ^{13}C NMR (100 MHz, DMSO-d_6): δ 20.57, 26.46, 50.43, 56.56 (2C), 104.69, 110.48, 110.51, 111.83, 111.90, 118.63, 118.84, 118.93, 121.50, 123.56, 123.67, 127.34, 130.67, 132.63, 132.65, 151.93, 152.02, 165.71, 168.31(2C); ESI-MS: *m/z* $[M]^+$ 488.51 (calcd 488.2); mp: 79 °C.

Cholinesterase Assay. Measurements of inhibitory activity against AChE and BuChE were performed using the Ellman method.[18]

Homology Modeling. Amino acid sequence for *Equus caballus* BuChE (horse BuChE, accession no: P81908) was obtained from UniProtKB (http://www.uniprot.org/). Template structure was searched on PSI-BLAST and sequence alignment with the selected template was performed using Discovery Studio (DS) 2016 (BIOVIA, San Diego, CA, USA). The homology model structure was generated by

using the *Build Homology Models* protocol available in DS. The energy minimization for the model structure was performed using GROMACS 5.0.6 package with CHARMM 27 force field. The steepest descent algorithm was used and the maximum number of minimization steps was set to 10 000. The stereochemical quality of the predicted structure was checked by PROCHECK[19] ProSA (Protein Structure Analysis),[20] and ERRAT.[21]

Molecular Docking Calculation. Molecular docking calculation of **11** to BuChE was performed using Genetic Optimization for Ligand Docking (GOLD) version 5.2.[22] The X-ray crystal structure of human BuChE (PDB ID: 4AQD)[23] from the RCSB Protein Data Bank (www.rcsb.org) and the homological model structure of horse BuChE were used. All co-crystal water and ligand molecules were removed from the structure. The protonation states of all titratable residues in the protein were set to pH 7 using *Clean Protein* tool in DS 2016. The 3D structure of **11** was prepared by DS. The geometry of the compound was optimized by energy minimization through *Minimize Ligands* tool in DS. All atoms within 15 Å from the center of the binding site were defined as docking sites. The number of docking runs was set to 100. The most populated conformations were selected for further investigation.

Molecular Dynamics Simulation. Molecular dynamics (MD) simulation of the protein-ligand complex was performed with AMBER03 force field[24] using GROMACS 5.0.6 package. The complex structure obtained from the molecular docking calculation was used as the initial structure for MD simulation. The ligand topology was generated by ACPYPE (AnteChamber Python Parser interface).[25] The complex structure was immersed in a water box of TIP3P water molecules[26] to make an aqueous environment. Counter-ions were added to neutralize the system and energy minimization with steepest descent algorithm was carried out until the maximum force converged to less than 1000 kJ/mol. The system was then subjected to 100 ps NVT equilibration followed by 100 ps NPT equilibration. Finally, a 10 ns production run was carried out under NPT ensemble. A constant temperature of 300 K and a pressure of 1 bar was controlled by Nose–Hoover thermostat[27] and Parrinello–Rahman barostat,[28] respectively. All bond lengths and the geometry of water molecules were restrained by LINCS[29] and SETTLE algorithms,[30] respectively. Cut-off values for short-range electrostatic and van der Waals interactions were 1.2 nm while long-range electrostatic interactions were calculated using particle mesh Ewald method.[31] The simulation was performed under periodic boundary conditions to avoid edge effects. The time step of the simulation was 2 fs and the coordinates were saved to trajectory files every 1 ps.

Results

Chemistry. The structures of tryptamine azide (**2**) and propargylated derivatives (**3**–**10**) of lipoic acid, polyphenols, and paeonol used in the click reactions are shown in Figure 2.

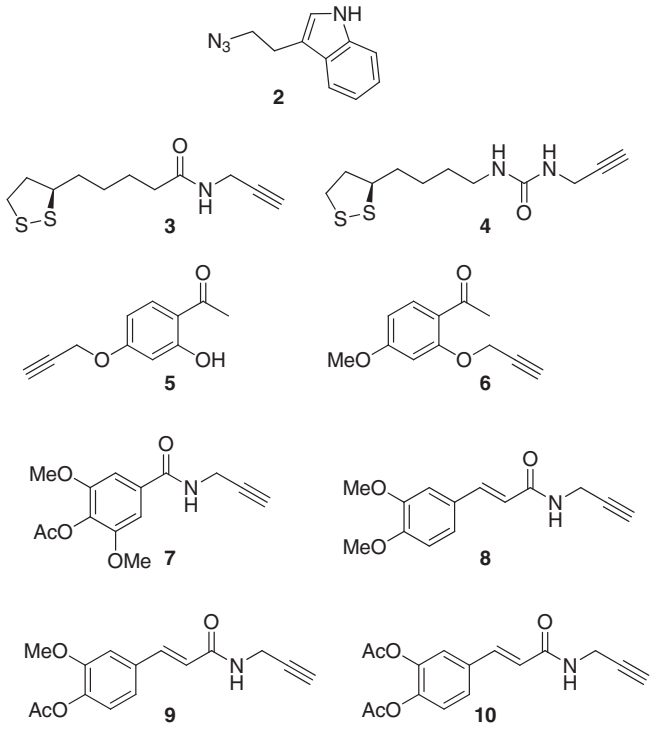

Figure 2. The structures of tryptamine azide and propargylated compounds prepared for click reaction.

The representative triazole-linked tryptamine derivatives **11**–**18** were, respectively, synthesized by the click reactions between tryptamine-azide (**2**) and the propargyl compounds **3**–**10** using a microwave reactor (Scheme 1). All tryptamine hybrid compounds synthesized in this work are listed in Figure 3.

Inhibitory Results (IC_{50} Value). The inhibitory effects (IC_{50} value) of tryptamine derivatives on AChE and BuChE are shown in Table 1 and galantamine was used as a

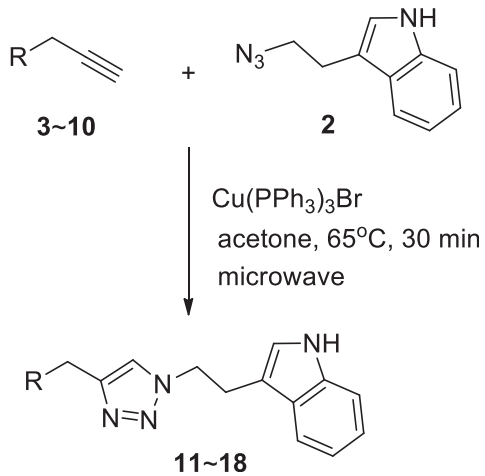

Scheme 1. Synthesis of triazole-linked tryptamine hybrid compounds by click reaction.

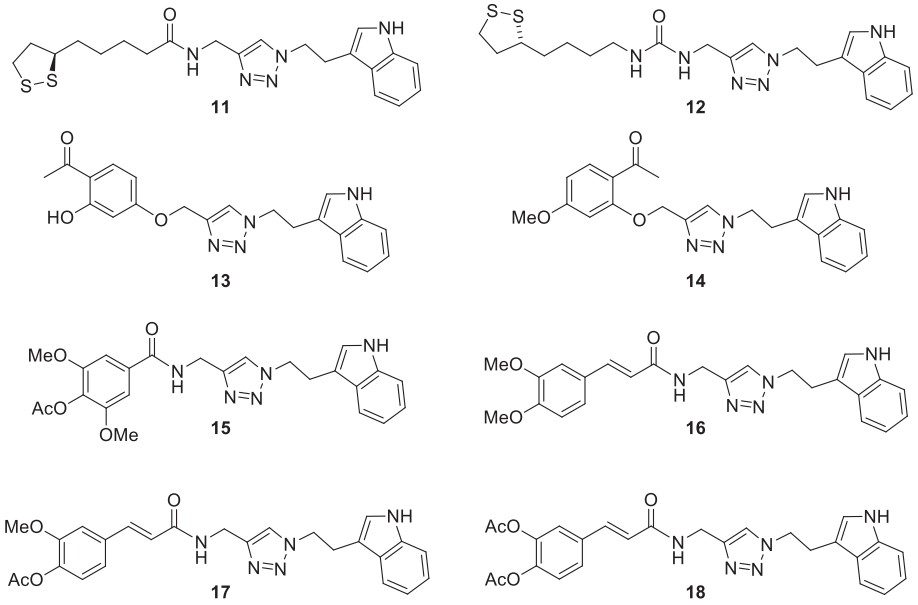

Figure 3. The structures of the triazol-linked tryptamine hybrid compounds synthesized in this work.

positive control compound. The starting compounds (tryptamine, lipoic acid, paeonol, syringic acid, ferulic acid, and caffeic acid) did not show any inhibitory effect for cholinesterases (data not shown). All tryptamine hybrid compounds had the same pattern as compound **1**. They selectively inhibited BuChE compared to AChE.

The Binding Mode of Compound 11 **in Horse BuChE.** *Homology Modeling of Horse (Equus caballus) BuChE.* A homology model of horse BuChE was constructed using the 3D structure of human BuChE as a template (PDB ID: 4AQD). Sequence alignment displayed that horse BuChE was highly homologous to human BuChE with a sequence identity of 90.2% and the similarity of 94.3% (Figure 4(a)).

Table 1. ChE inhibition IC_{50} values for tryptamine hybrid compounds.[a]

Sample	LogP value[c]	AChE inh. IC_{50}(μM)	BuChE inh. IC_{50}(μM)
Gal.	1.41	0.64 ± 0.1	8.4 ± 0.1
1	3.88	91.30 ± 0.97	0.72 ± 0.11
11	3.32	>480	0.42 ± 0.29
11[b]		>480	1.96 ± 0.15
±**12**	2.98	>480	7.69 ± 0.82
13	2.48	229.8 ± 1.26	>450
14	2.75	>450	5.49 ± 0.41
15	2.16	>450	9.04 ± 0.62
16	2.92	>450	>450
17	2.63	>450	41.79 ± 1.30
18	2.34	>450	>450

[a] AChE (from electric eel) and BuChE (from horse serum) were used. [b] BuChE (from human serum). IC_{50} values represent the inhibitor concentration necessary to decrease enzyme activity by 50% and are calculated using the mean of the triplicate measurements. [c] LogP values were calculated by using ChemDraw Program.

The structural alignment of horse BuChE to the template showed that the overall tertiary structures are very similar with a root-mean-square deviation (RMSD) of 0.16 Å for the backbone atoms in the proteins (Figure 4(b)). They shared the same active site residues, except that Ala277 of human BuChE is replaced by Val277 in horse BuChE. The homology model was subjected to energy minimization to refine intramolecular contacts followed by the assessment of its stereochemical quality. Ramachandran plot from PROCHECK revealed that 91.2% of the residues were in the most favored regions, 8.4% were in additional allowed regions, and only two residues were found in disallowed regions (Figure 4(c)). The ProSA *Z*-Score value of −10.6 was within the range of scores typically found for native proteins of similar size. Moreover, a quality factor score obtained from ERRAT was 95.93, which represents a high quality model (Figure 4(d)). As a result, the quality of our homology model for horse BuChE was evaluated using three different criteria. These results indicated that the model structure is reliable for further modeling studies.

Binding Conformation of ***11*** *at the Active Site of Horse BuChE.* Molecular docking of **11** to horse BuChE was also performed. The GOLD fitness score for all the generated 100 poses ranged from 59.08 to 82.1. The result showed that 62 conformations were similar to that of human BuChE. The top-scored conformation was selected as a starting structure for MD simulation. To check the stability of the system, RMSD and potential energies were measured during the 10 ns simulation time. The C_α RMSD value for the protein and the potential energies were constant and remained less than 0.15 nm and −1 030 000 kJ/mol, respectively (Figure 5(a) and (b)). Structural analysis revealed that the binding mode of **11** in horse BuChE was analogous to that of human BuChE (Figure 5(c) and (d)).

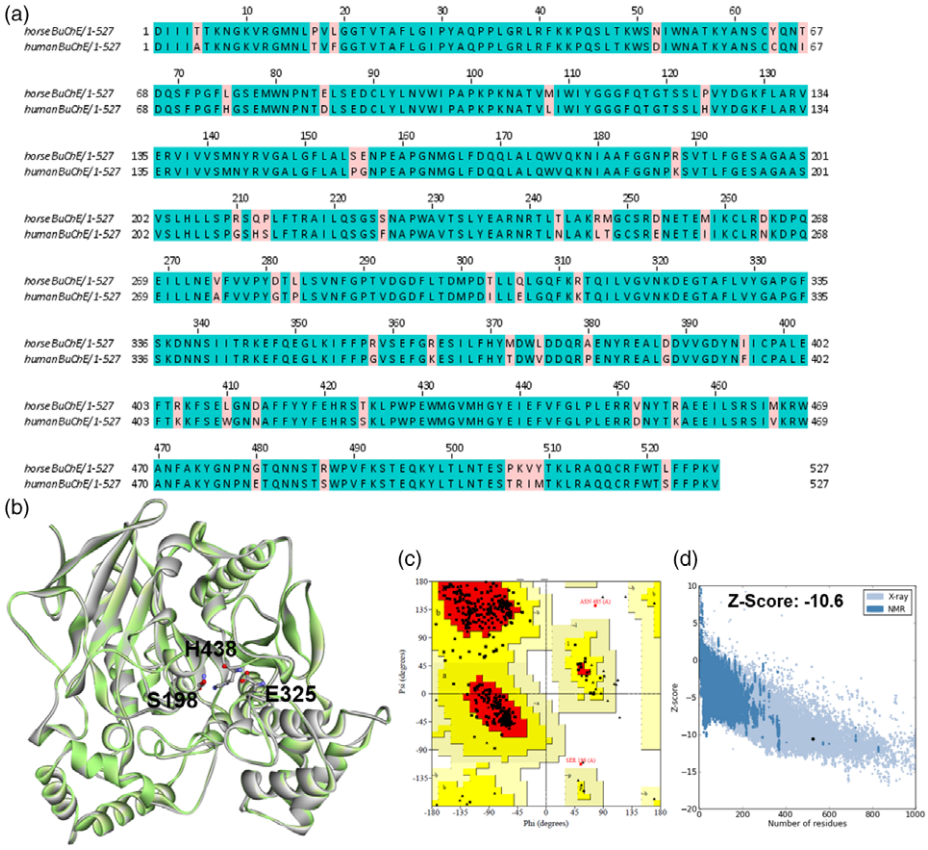

Figure 4. Homology modeling for horse BuChE. (a) Sequence alignment between horse and human BuChEs. (b) Superimposed structure of homology model (green) and template (gray) of BuChE. The catalytic triad of horse BuChE was displayed as gray stick models. (c) Ramachandran plot of the backbone dihedral angles (φ and ψ) for the model structure of horse BuChE. (d) ProSA plot of model structure. The *Z*-score of −10.6 was represented as a black dot.

*Binding Conformation of **11** at the Active Site of Human BuChE.* Molecular docking calculation was performed to explore the binding mode of **11** in the active site of human BuChE. From the top cluster including 48 out of 100 docking poses, a pose with a GOLD fitness score of 80.45 was selected as a representative pose of the compound based on their molecular interactions (Figure 6). The binding conformation of **11** showed that the indole group of the compound was headed for Trp82 and the end of lipoamide group was toward to Ser198. The complex structure was subjected to MD simulation in order to alleviate unfavorable contacts and check the binding stability. Prior to trajectory analysis, the RMSD for the C_α atoms in the protein and the potential energy of the system were calculated. The RMSD was converged within 0.15 nm during 10 ns MD simulation (Figure 7(a)). The potential energy was also maintained at about −1 075 000 kJ/mol (Figure 7(b)). Both plots showed that there were no abnormal behaviors in the structure during the entire simulation time. A snapshot with the lowest potential energy was taken as a representative structure for further analysis. Compound **11** bound to human BuChE by forming a hairpin or U-shaped structure in the active site (Figure 7(c) and (d)).

Discussion

Compound **11** exhibited slightly higher inhibitory activity against BuChE (from horse serum, $IC_{50} = 0.42 \pm 0.29$ μM) than compound **1**. The IC_{50} value (1.96 ± 0.15 μM) was a little higher for the BuChe originating from human serum compared to horse serum. Molecular modeling study for BuChE originating from both human and horse were also done on compound **11**.

Lipoic acid transferred to compound **4**, which has one less carbon, through Curtius rearrangement reaction quenching with propargyl amine. The click reaction between **4** and **2** resulted in compound **12** ($IC_{50} = 7.69 \pm 0.82$ μM). Compound **11**, which has an amide functional group, had an IC_{50} value 10 times less than compound **12**, which has an urea functional group.

Compounds **13** and **14** are derivatives of paeonol. When anti-inflammatory activity was measured using compounds **13**, **14,** and **15**, compound **13** and **14** independently inhibited NO (nitric oxide) production in BV2 cells. However, compound **15** suppressed NO generation to a minimum. This means that the paeonol moiety plays an important role in the anti-inflammatory effect.[17] Starting

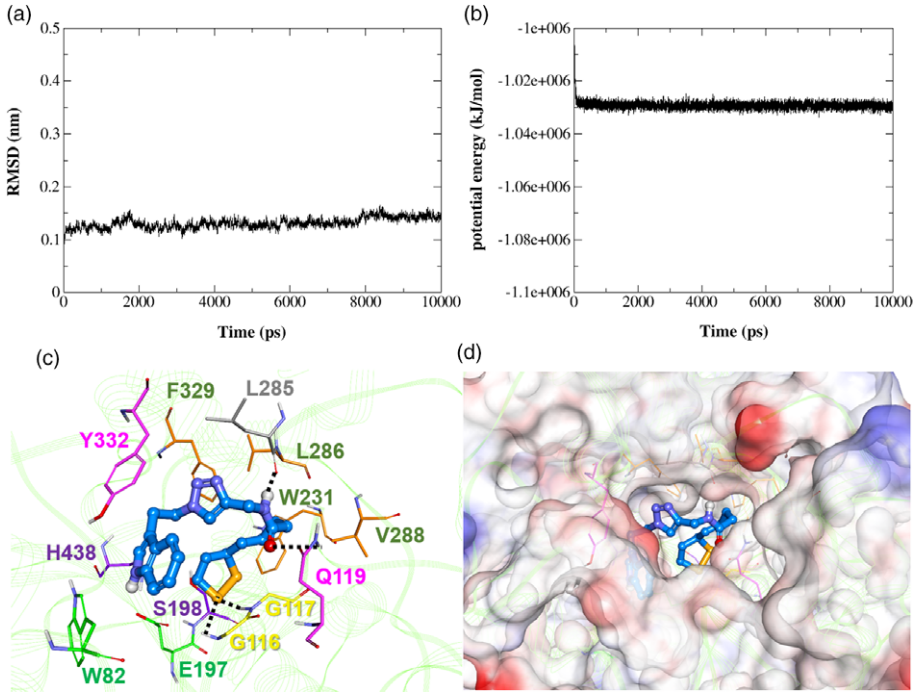

Figure 5. The results of 10 ns MD simulation for horse BuChE in complex with compound **11**. (a) The RMSD of C_α atoms and (b) potential energy were calculated during the simulation time. (c) Detailed binding mode of compound **11** at the active site of horse BuChE. The protein and compound **11** were shown as green line ribbons and blue stick models, respectively. The active site residues were displayed as different stick colors based on their subsites, PAS (magenta), ABP (orange), OH (yellow), CAS (purple), and AS (green), respectively. The residues not belonging to any subsite were shown as gray stick models. Hydrogen bonds were represented as black dashed lines. (d) The surface representation for **11** binding in horse BuChE. The protein surface was colored by its electrostatic potential (blue, positive; red, negative).

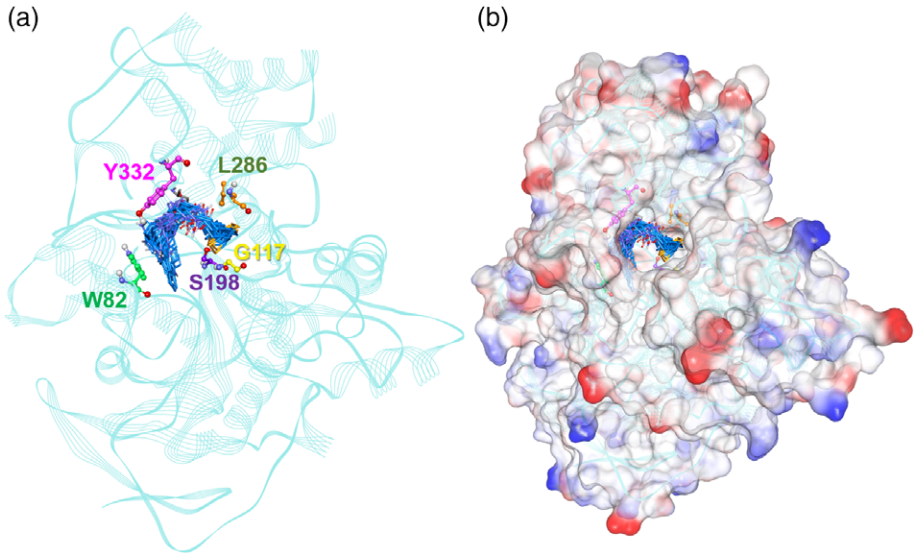

Figure 6. The most populated conformations of compound **11** in human BuChE. (a) Binding pattern of **11** in the active site of human BuChE. The protein and the compound were drawn as sky blue line ribbons and blue stick models. The active site residues were displayed as different stick colors based on their subsites, PAS (magenta), ABP (orange), OH (yellow), CAS (purple), and AS (green), respectively. (b) The docking poses for compound **11** were shown with the electrostatic potential surface of human BuChE (blue, positive; red, negative).

compound **5** was synthesized from the selective propargylation between 2,4-dihydroxyacetophenone and propargyl chloride, which replaced the methyl group of 4-methoxy group of paeonol with a propargyl group. Starting compound **6** was obtained from the propargylation of paeonol. Compounds **13** and **14** were synthesized by the

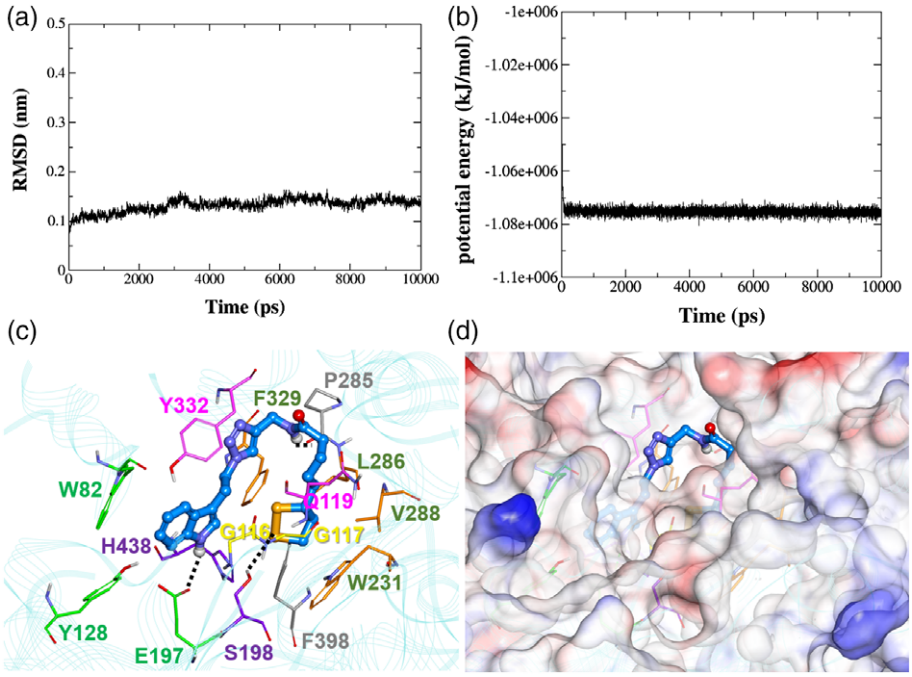

Figure 7. The results of 10 ns MD simulation for human BuChE in complex with compound **11**. (a) The RMSD of C_α atoms and (b) potential energy were calculated during the simulation time. (c) Detailed binding mode of compound **11** at the active site of human BuChE. The protein and compound **11** were shown as sky blue line ribbons and blue stick models, respectively. The active site residues displayed as different stick colors based on their subsites, PAS (magenta), ABP (orange), OH (yellow), CAS (purple), and AS (green), respectively. The residues not belonging to any subsite were shown as gray stick models. Hydrogen bonds were represented as black dashed lines. (d) The surface representation for **11** binding in human BuChE. The protein surface was colored by its electrostatic potential (blue, positive; red, negative).

click reactions between compounds **5** or **6** and tryptamine azide, respectively. Compound **13** exhibited weak inhibitory activity against AChE, but there was no inhibitory activity against BuChE. Compound **14** showed moderate inhibitory activity against BuChE only (IC_{50} = 5.49 ± 0.41 μM). Compounds **15–18** coupled between tryptamine azide and propargylated polyphenols such as acetyl syringic acid, 3,4-dimethoxy cinnamic acid, acetyl ferulic acid, and diacetyl caffeic acid showed moderate or no inhibitory activity against BuChE. This may be due to the size effect of polyphenol. Compound **15** has the benzoic acid moiety, but compounds **16–18** have the cinnamic acid moiety. The size of cinnamic acid is bigger than that of benzoic acid. When anti-inflammatory activity was measured using compounds **13**, **14,** and **15**, compound **13** and **14** showed similar inhibitory effects on LPS-induced NO production, while compound **15** had little anti-inflammatory activity. However, compound **14** was less cytotoxic than **13**.[17] In the measurement of cholinesterase inhibitory activity using these compounds, compound **13** weakly inhibited AChE, while compounds **14** and **15** selectively inhibited BuChE.

Previous we synthesized hybrid molecules between (*R*)-lipoic acid (ALA) and acetylated or methylated polyphenol compounds and evaluated their *in vitro* cholinesterases [acetylcholinesterase (AChE) and butyrylcholinesterase (BuChE)] inhibitory activity.[32] In ALA-polyphenol compounds, ALA-acetylated caffeic acid compounds showed the highest BuChE inhibitory activity, while in the tryptamine derivatives acetylated syringic acid derivative showed the highest activity. In ALA-polyphenol compounds, activity was analyzed using various QSAR parameters [hydrophobicity parameter (π), Hammett electronic substituent constant (σm & σp), and molar refractivity (MR)].[32]

In the tryptamine derivative, the size of the propargyl moiety and the position of its functional group appear to be important for anti-inflammatory activity and cholinesterase inhibitory activity.

The binding mode of compound **11** was analyzed. It was observed that the indole group interacted with Trp82 and Tyr332 though π–π stacking interactions with horse BuChE. The middle triazole ring also formed π–π stacking with Phe329. The lipoamide group was stabilized by hydrophobic interactions with the active site residues including Glu197, Ser198, Trp231, Leu285, Leu286, and Val288. The middle NH moiety and carbonyl group in lipoamide group made hydrogen bonds with Leu285 and Gln119, respectively. Furthermore, the sulfur atom in a terminal dithiolane ring of lipoamide group formed hydrogen bond interactions with Gly116 and Gly117. The middle amide group of compound **11** was toward the outside, and indole

and lipoamide groups at both ends were buried inside of human BuChE. The indole group of compound **11** was placed near a catalytic anionic site (CAS) and anionic subsite (AS). It showed hydrophobic interactions with Trp82 and Tyr128 on the AS and His438 on the CAS. The NH group of the indole ring formed a hydrogen bond with the carboxyl group of Glu197. On the other hand, the lipoamide group was positioned within the pocket surrounded by residues that belong to the peripheral anionic subsite (PAS), acyl binding pocket (ABP), and oxyanion hole (OH). It formed hydrophobic interactions with Gln119 and Tyr332 on PAS, Leu286, Val288, and Trp231 on ABP, as well as Gly116 and Gly117 on OH subsites. Additionally, a terminal dithiolane ring in the lipoamide group was involved in sulfur-π interactions with Phe329 and Phe398. The middle NH moiety and sulfur atom in the dithiolane ring were hydrogen bonded to the backbone carbonyl group of Pro285 and the hydroxyl group of Ser198, one of the catalytic triad, respectively.

A kinetic study of BuChE was performed at different concentrations of compound **11** to explore inhibition mechanisms (Figure 8), and the Lineweaver–Burk plot suggested a mixed type of inhibition. The mixed type of inhibition corresponds well with the molecular modeling study, in which compound **11** was bound to the CAS, AS, PAS, ABP, and OH.

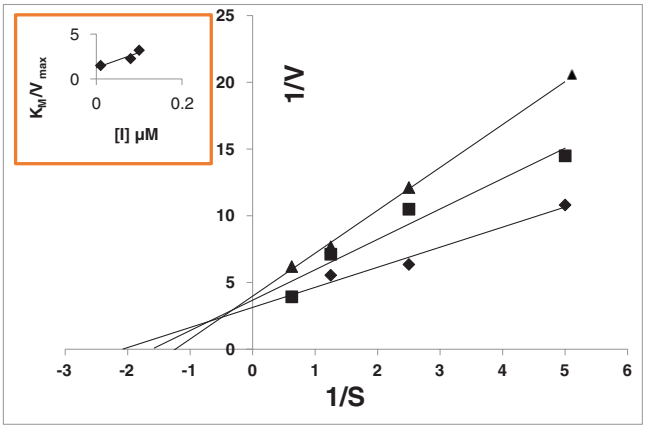

Figure 8. Lineweaver–Burk plot of the kinetic study of the inhibitory effect of compound **11** against BuChE (◆ = 001 μM, ▲ = 0.08 μM, ▲ = 0.10 μM). The inset is a plot of [I] *vs.* K_M/V_{max}.

Conclusion

In conclusion, a series of tryptamine–triazole hybrid compounds **11–19** were synthesized via click reactions between tryptamine azide and propargylated derivatives. They generally showed butyrylcholinesterase inhibitory activity. Compound **11** showed the most potent inhibitory activity (IC_{50} = 0.42 ± 0.29 for equine BuChE and 1.96 ± 0.15 for human BuChE) among the 10 compounds and its inhibitory mechanism against BuChE was a mixed type of inhibition.

In order to investigate the binding mode of compound **11** to the active site of human and horse BuChE, molecular docking and MD simulation was performed using human BuChE determined by crystal structure and horse BuChE generated by homology modeling. The results indicate that the binding pattern of compound **11** is almost identical in both structures. Compound **11** forms hydrogen bond interactions with Glu197, Ser198, and Pro285 in human BuChE while compound **11** interacts with Gly116, Gly117, Gln119, and Leu285 in horse BuChE. The detailed structural analysis demonstrates that compound **11** is bound to the active site by forming various molecular interactions with the residues across all the subsites in both human and horse BuChEs. Taken together, our molecular modeling studies provide valuable information to design potential inhibitors of BuChE.

Acknowledgments. This research was supported by the Next-Generation BioGreen 21 Program (PJ01106202) from Rural Development Administration (RDA) of Republic of Korea and by Basic Science Research Program through the National Research Foundation of Korea (NRF) funded by the Ministry of Education (2017R1D1A1B04028757).

References

1. J. Godyń, J. Jończyk, D. Panek, B. Malawska, *Pharmacol. Rep.* **2016**, *68*, 127.
2. P. T. Francis, A. M. Palmer, M. Snape, *J. Neurol. Neurosurg. Psychiatry* **1999**, *66*, 137.
3. S. Darvesh, D. L. Grantham, D. A. Hopkins, *J. Comp. Neurol.* **1998**, *393*, 374.
4. N. H. Greig, T. Utsuki, D. K. Ingram, Y. Wang, G. Pepeu, C. Scali, Q. S. Yu, J. Mamczarz, H. W. Hollway, T. Giordano, D. Chen, K. Furukawa, K. Sambamurti, A. Brossi, D. K. Lahiri, *Proc. Natl. Acad. Sci. USA* **2005**, *102*, 17213.
5. B. C. Scott, O. I. Aruoma, P. J. Evans, C. O'Neill, A. Van der Vliet, C. E. Cross, H. Trischler, B. Halliwell, *Free Radic. Res.* **1994**, *20*, 119.
6. J. L. Evans, I. D. Goldfine, *Diabetes Technol. Ther.* **2000**, *2*, 401.
7. M. Rosini, V. Andrisano, M. Bartolini, M. L. Bolognesi, P. Hrelia, A. Minarini, A. Tarozzi, C. Melchiorre, *J. Med. Chem.* **2005**, *48*, 360.
8. L. Jalili-Baleh, H. Forootanfar, T. T. Küçükkılınç, H. Nadri, Z. Abdolahi, A. Ameri, M. Jafari, B. Ayazgok, M. Baeeri, M. Rahimifard, S. N. Abbas Bukhari, M. Abdollahi, M. R. Ganjali, S. Emami, M. Khoobi, A. Foroumadi, *Eur. J. Med. Chem.* **2018**, *152*, 600.
9. Y. Mei, D. Wei, J. Liu, *Cancer Biol. Ther.* **2005**, *4*, 468.
10. M. F. Muldoon, S. B. Kritchevsky, *BMJ* **1996**, *312*, 458.
11. O. Vieira, I. Escargueil-Blanc, O. Meilhac, J. P. Basile, J. Laranjinha, L. Almeida, R. Salvayre, A. Nègre-Salvayre, *Br. J. Pharmacol.* **1998**, *123*, 565.
12. Y. Fukuhara, D. Yoshida, *Agric. Biol. Chem.* **1987**, *51*, 1441.
13. (a) Y. Ou, Q. Li, J. Wang, K. Li, S. Zhou, *Biomol. Ther. (Seoul)* **2014**, *22*, 341. (b) T.-C. Chou, *Br. J. Pharmacol.* **2003**, *139*, 1146.

14. J. Y. Park, S. Shin, J. K. Kim, K. C. Park, J. H. Park, *Bull. Kor. Chem. Soc.* **2016**, *37*, 1464.
15. E. D. Goddard-Borger, R. V. Stick, *Org. Lett.* **2007**, *9*, 3797.
16. R. Gujadhur, D. Venkataraman, *Synth. Commun.* **2001**, *31*, 2865.
17. E. H. Jung, J. S. Hwang, M. Y. Kwon, K. H. Kim, H. Cho, I. K. Lyoo, S. Shin, J. H. Park, I. O. Han, *Neurochem. Int.* **2016**, *100*, 35.
18. G. I. Ellman, K. D. Coutney, V. Andres, R. M. Feather-stone, *Biochem. Pharmacol.* **1961**, *7*, 88.
19. R. A. Laskowski, M. W. MacArthur, D. S. Moss, J. M. Thornton, *J. Appl. Crystallogr.* **1993**, *26*, 283.
20. (a) M. J. Sippl, *Proteins* **1993**, *17*, 355. (b) M. Wiederstein, M. J. Sippl, *Nucleic Acids Res* **2007**, *35*, W407.
21. C. Colovos, T. O. Yeates, *Protein Sci.* **1993**, *2*, 1511.
22. (a) G. Jones, P. Willett, R. C. Glen, A. R. Leach, R. Taylor, *J. Mol. Biol.* **1997**, *267*, 727. (b) M. L. Verdonk, J. C. Cole, M. J. Hartshorn, C. W. Murray, R. D. Taylor, *Proteins* **2003**, *52*, 609.
23. X. Brazzolotto, M. Wandhammer, C. Ronco, M. Trovaslet, L. Jean, O. Lockridge, P. Y. Renard, F. Nachon, *FEBS J.* **2012**, *279*, 2905.
24. Y. Duan, C. Wu, S. Chowdhury, M. C. Lee, G. Xiong, W. Zhang, R. Yang, P. Cieplak, R. Luo, T. Lee, J. Caldwell, J. Wang, P. Kollman, *J. Comput. Chem.* **2003**, *24*, 1999.
25. A. W. Sousa da Silva, W. F. Vranken, *BMC. Res. Notes* **2012**, *5*, 367.
26. W. L. Jorgensen, J. Chandrasekhar, J. D. Madura, R. W. Impey, M. L. Klein, *J. Chem. Phys.* **1983**, *79*, 926.
27. (a) S. Nosé, M. Klein, *Mol. Phys.* **1983**, *50*, 1055. (b) W. G. Hoover, *Phys. Rev. A* **1985**, *31*, 1695.
28. M. Parrinello, A. Rahman, *J. Appl. Phys.* **1981**, *52*, 7182.
29. (a) J. P. Ryckaert, G. Ciccotti, H. J. C. Berendsen, *J. Comput. Phys.* **1977**, *23*, 327. (b) B. Hess, H. Bekker, H. J. C. Berendsen, J. G. E. M. Fraaije, *J. Comput. Chem.* **1997**, *18*, 1463.
30. S. Miyamoto, P. A. Kollman, *J. Comput. Chem.* **1992**, *13*, 952.
31. (a) T. Darden, D. York, L. Pedersen, *J. Chem. Phys.* **1993**, *98*, 10089. (b) U. Essmann, L. Perera, M. L. Berkowitz, T. Darden, H. Lee, L. G. Pedersen, *J. Chem. Phys.* **1995**, *103*, 8577.
32. Y. J. Woo, B. H. Lee, G. H. Yeun, H. J. Kim, J. M. Ko, M.-H. Won, B. H. Lee, J. H. Park, *Bull. Kor. Chem. Soc.* **2011**, *32*, 2997.

